

With or without spikes: localization of focal epileptic activity by simultaneous electroencephalography and functional magnetic resonance imaging

Frédéric Grouiller,¹ Rachel C. Thornton,² Kristina Groening,³ Laurent Spinelli,¹ John S. Duncan,² Karl Schaller,⁴ Michael Siniatchkin,^{3,5} Louis Lemieux,² Margitta Seeck,¹ Christoph M. Michel¹ and Serge Vulliemoz^{1,2}

1 Presurgical Epilepsy Evaluation Unit and Functional Brain Mapping Laboratory, Neurology Department, University Hospital, University of Geneva, 1 Geneva, Switzerland

2 Department of Clinical and Experimental Epilepsy, UCL Institute of Neurology and Epilepsy Society, London, WC1N 3BG, UK

3 Department of Paediatric Neurology, Children's Hospital, Christian-Albrechts-University of Kiel, 24098 Kiel, Germany

4 Department of Neurosurgery, University Hospital, University of Geneva, 1211 Geneva, Switzerland

5 Department of Children and Adolescents Psychiatry and Psychotherapy, Philipps-University of Marburg, 35037 Marburg, Germany

Correspondence to: Dr Serge Vulliemoz,
Epilepsy Unit, Neurology Department,
University Hospital of Geneva,
4 rue Gabrielle-Perret-Gentil,
1211 Geneva 4,
Switzerland
E-mail: serge.vulliemoz@hcuge.ch

In patients with medically refractory focal epilepsy who are candidates for epilepsy surgery, concordant non-invasive neuroimaging data are useful to guide invasive electroencephalographic recordings or surgical resection. Simultaneous electroencephalography and functional magnetic resonance imaging recordings can reveal regions of haemodynamic fluctuations related to epileptic activity and help localize its generators. However, many of these studies (40–70%) remain inconclusive, principally due to the absence of interictal epileptiform discharges during simultaneous recordings, or lack of haemodynamic changes correlated to interictal epileptiform discharges. We investigated whether the presence of epilepsy-specific voltage maps on scalp electroencephalography correlated with haemodynamic changes and could help localize the epileptic focus. In 23 patients with focal epilepsy, we built epilepsy-specific electroencephalographic voltage maps using averaged interictal epileptiform discharges recorded during long-term clinical monitoring outside the scanner and computed the correlation of this map with the electroencephalographic recordings in the scanner for each time frame. The time course of this correlation coefficient was used as a regressor for functional magnetic resonance imaging analysis to map haemodynamic changes related to these epilepsy-specific maps (topography-related haemodynamic changes). The method was first validated in five patients with significant haemodynamic changes correlated to interictal epileptiform discharges on conventional analysis. We then applied the method to 18 patients who had inconclusive simultaneous electroencephalography and functional magnetic resonance imaging studies due to the absence of interictal epileptiform discharges or absence of significant correlated haemodynamic changes. The concordance of the results with subsequent intracranial electroencephalography and/or resection area in patients who were seizure free after surgery was assessed. In the validation group, haemodynamic changes correlated to voltage maps were similar to those obtained with conventional analysis in 5/5 patients. In 14/18 patients (78%) with previously inconclusive studies, scalp

maps related to epileptic activity had haemodynamic correlates even when no interictal epileptiform discharges were detected during simultaneous recordings. Haemodynamic changes correlated to voltage maps were spatially concordant with intracranial electroencephalography or with the resection area. We found better concordance in patients with lateral temporal and extratemporal neocortical epilepsy compared to medial/polar temporal lobe epilepsy, probably due to the fact that electroencephalographic voltage maps specific to lateral temporal and extratemporal epileptic activity are more dissimilar to maps of physiological activity. Our approach significantly increases the yield of simultaneous electroencephalography and functional magnetic resonance imaging to localize the epileptic focus non-invasively, allowing better targeting for surgical resection or implantation of intracranial electrode arrays.

Keywords: epilepsy; EEG–fMRI; EEG maps; long-term EEG monitoring

Abbreviations: BOLD = blood oxygen level dependent; FWE = family-wise error

Introduction

Thirty to 40% of the patients with focal epilepsy have medically refractory seizures and should be evaluated for the possibility of epilepsy surgery, which can have a life-changing impact (Spencer and Huh, 2008). In recent years, the improvement of non-invasive imaging techniques has led to a better understanding of epileptic networks and epilepsy surgery is now considered in an increasing number of patients (Duncan, 2010).

Simultaneous electroencephalography (EEG) and functional magnetic resonance imaging (MRI) recordings allow the mapping of haemodynamic changes that correlate with specific physiological or pathological electrophysiological features identified on EEG (Gotman, 2008). In patients with epilepsy, whole-brain high-resolution functional MRI maps of blood oxygenation level-dependant (BOLD) signal changes related to interictal epileptiform discharges (spikes) can be obtained. This information can then be used to help to identify targets for surgical resection or implantation of intracranial EEG electrodes in surgical candidates (Zijlmans *et al.*, 2007; Moeller *et al.*, 2009).

In 40–70% of EEG–functional MRI recordings in patients with focal epilepsy, no significant spike-related BOLD changes are observed (Aghakhani *et al.*, 2006; Salek-Haddadi *et al.*, 2006; Gotman, 2008). The reasons are two-fold: in many patients, the absence of spikes during functional MRI acquisition precludes statistical analysis, while in other patients, there may be no significant spike-related BOLD changes. Given these limitations, alternative methods to infer BOLD changes related to epileptic activity have been explored but have only been applied to studies with spikes (Liston *et al.*, 2006; Jann *et al.*, 2008; Vulliemoz *et al.*, 2009a). Only a fraction of cortical spikes recorded with intracranial electrodes can be identified on simultaneous scalp EEG recordings (Alarcon *et al.*, 1994; Tao *et al.*, 2005). However, the pathological activity not detected on scalp EEG may be associated with haemodynamic changes detectable using functional MRI (Vulliemoz *et al.*, 2011).

EEG is conventionally analysed as waveforms over multiple channels and spikes are defined by characteristic morphological features in this display. Absence of spikes in the EEG means that none of these features have been visually detected. In addition to the display of multiple EEG waveforms, electrical activity recorded with scalp EEG can be represented by scalp voltage topographic

maps (EEG maps). These topographic maps reflect the momentary activity of neuronal networks via the summation of post-synaptic cortical potentials over the whole brain. Changes in the activity of focal electrical brain generators will influence the topography of these maps ('forward model') (Michel *et al.*, 2004b). It has been shown that these maps can reflect the electrical generators of focal epileptic activity (Ebersole and Wade, 1990; Lopes da Silva, 1990). We postulate that the occurrence of these epilepsy-specific EEG maps in the resting EEG of individual patients represents an increase in the activity of the epileptic sources and could allow the detection of sub-threshold activity even in the absence of visually identifiable epileptic waveforms on the conventional EEG.

To test this hypothesis, we have developed an innovative approach that does not require identifiable spikes during functional MRI to reveal BOLD changes related to epileptic activity. We built patient-specific EEG maps of the epileptic activity derived from spikes detected in the long-term clinical video-EEG monitoring (long-term EEG) outside the scanner. We then calculated the strength of the presence of these maps in the EEG recorded during functional MRI as a function of time using correlation. Finally, we used this correlation coefficient to inform functional MRI analysis and detect topography-related BOLD changes. We initially validated the method in patients with spikes during functional MRI by comparing the topography-related BOLD changes with conventional analysis of spike-related BOLD changes. We then applied our method in patients in whom previous EEG–functional MRI analysis with conventional analysis had been inconclusive (no spike or no spike-related BOLD changes). Subsequent intracranial EEG recordings or area of surgical resection were used to validate our results.

Materials and methods

Patients

Patients with refractory focal epilepsy were selected from EEG–functional MRI databases in three centres: the Neurology Department of Geneva University Hospital (Switzerland), UCL Institute of Neurology, the National Hospital for Neurology and Neurosurgery and the

Epilepsy Society (London, UK) and the Department of Paediatric Neurology of Kiel University Hospital (Germany).

All patients and the parents of paediatric patients gave written informed consent and the EEG–functional MRI procedure was approved by the local ethics committee of the three research centres.

Study design

A group of five patients was used for the validation of our method. These patients had statistically significant focal spike-related BOLD changes [$P < 0.05$, family-wise error (FWE) corrected for multiple comparisons]. Clinical description of these patients is given in Table 1.

In the second part of the study, we selected patients ($n = 20$) with previously inconclusive EEG–functional MRI studies corresponding to the following inclusion criteria: (i) absence of spikes on EEG–functional MRI or absence of spike-related BOLD changes with conventional analysis; (ii) detectable spikes during long-term EEG; and (iii) an epileptic focus unequivocally defined by subsequent intracranial EEG and/or seizure freedom following postoperative resection according to Engel's outcome scale (Engel *et al.*, 1993). Clinical description of these patients is given in Table 2.

Long-term clinical video-electroencephalography monitoring

All patients underwent presurgical evaluation including long-term EEG with 20–40 scalp electrodes placed according to the 10–10 electrode position convention following local protocols (Geneva: 29 electrodes, London: 18–24 electrodes, Kiel: 37–40 electrodes) with EEG sampling rates of 256 or 512 Hz.

Electroencephalography–functional magnetic resonance imaging acquisition

Patients underwent simultaneous EEG–functional MRI recordings between 15 and 30 min at rest with eyes closed. A 32, 64 or 96 magnetic resonance-compatible EEG cap (EasyCaps, FalkMinnow Services) was used according to the 10–10 system. Electrodes were equipped with an additional 5 k Ω resistance and impedances were kept as low as possible. EEG was acquired at 5 kHz using 1–3 BrainAmp magnetic resonance-compatible amplifiers (Brain Products) and EEG was synchronized with the MRI clock. Some of the children (Patients 7,

18 and 19) were sedated for the procedure following a routine procedure reported in previous publications (Jacobs *et al.*, 2008a; Groening *et al.*, 2009).

Functional MRI was acquired using a T_2^* -weighted single-shot gradient-echo echo-planar images with a 3-Tesla magnetic resonance scanner (Geneva: Siemens Magnetom Trio, 12-channel head receive coil with body transmit coil; London: Signa Excite HDX, GE Medical Systems, quadrature transmit and receive headcoil; Kiel: Philips Achieva, Philips, eight-channel head receive coil with body transmit coil). Five different echo planar imaging sequences were used depending on the centre and the date of data acquisition: (i) Geneva: repetition time = 1200 ms, voxel size: $3.75 \times 3.75 \times 5.5 \text{ mm}^3$, 25 slices (Patients 4 and 6); (ii) Geneva: repetition time = 1500 ms, voxel size: $3.75 \times 3.75 \times 5.5 \text{ mm}^3$, 25 slices (Patients 1, 3, 5, 10, and 13–16); (iii) Geneva: repetition time = 1980 ms, voxel size: $3 \times 3 \times 3.75 \text{ mm}^3$, 32 slices (Patient 11); (iv) Kiel: repetition time = 2250 ms, voxel size: $3.125 \times 3.125 \times 3.8 \text{ mm}^3$, 30 slices (Patients 7 and 17–19); (v) London: repetition time = 3000 ms, voxel size: $3.75 \times 3.75 \times 3 \text{ mm}^3$, 43 slices (Patients 2, 8, 9, 12 and 20–25).

Processing of the electroencephalography recorded during functional magnetic resonance imaging

Gradient and pulse artefacts (i.e. all artefacts time-locked to cardiac activity) were removed from the EEG with Vision Analyser (Version 1.05, Brain Products), using average artefact subtraction methods (Allen *et al.*, 1998, 2000). The EEG was down-sampled to 250 Hz after gradient artefact correction. If necessary, residual artefacts were removed with temporal independent component analysis of the EEG using the Infomax approach (Bell and Sejnowski, 1995): independent components corresponding to pulse artefacts, eye-blink or residual scanner artefacts were identified by visual inspection of independent component analysis components' time courses and removed before back projection.

Topography-based analysis

Figure 1 describes the steps of the topography-related analysis detailed below. The magnetic resonance-corrected EEG was processed using Cartool software (Brunet *et al.*, 2011).

For each patient, spikes were marked on a representative segment of long-term EEG by an experienced neurophysiologist (S.V.) and the spike types congruent with electroclinical semiology were selected

Table 1 Validation group: clinical details of patients with significant spike-related BOLD changes

Patients	Age/age of onset/gender	Localization	Cause	Scalp EEG focus	icEEG	Resection
1	13/1/F	Left frontal	Tuberous sclerosis	Left frontotemporal	+	Left prefrontal tuber
2	37/6/F	Left frontal	Unspecific white matter lesion	Left > right frontal	+	Left superior frontal cortectomy
3	7/3/M	Left fronto-temporal	Gliosis post-bacterial abscess	Left frontal	+	Left fronto-temporo-parietal cortectomy
4	12/3/M	Right parietal	Complex right hemispheric malformation	Temporo-occipital	–	–
5	8/7/M	Left parieto-occipital	DNT	Bilateral parieto-occipital	–	Lesionectomy

DNT = dysembryoplastic neuroepithelial tumour; icEEG = intracranial EEG; M/F = male/female.

Table 2 Clinical details of patients with previously inconclusive EEG–functional MRI (absence of significant spike-related BOLD changes)

Patients	Age/age of onset/ gender	Focus side	Localization	Cause	Scalp EEG focus	icEEG	Resection	Outcome	Follow-up (months)
6	13/7/F	Left	Frontal	Left frontocentral FCD	Left frontocentral	–	Lesionectomy	Ia	>12
7	4/2/M	Left	Frontal	FCD	Left > Right frontal	–	Lesionectomy	Ia	>12
8	27/15/M	Left	Frontal	Post-traumatic	Left frontocentral	+	Left middle frontal cortectomy	Ia	>12
9	23/3/F	Left	Frontal	FCD	Left prefrontal	+	Lesionectomy left superior frontal	Ia	>12
10	6/4/F	Left	Insula	Probable FCD	Left centroparietal slowing	–	Left insular corticectomy	Ia	>12
11	26/4/F	Left	Parietal	Gliosis post-meningoencephalitis	Left parieto-occipital	+	Left parietooccipital	Ia	3
12	18/7/F	Right	Parietal	FCD	Midline	+	Right medial parietal	Ia	>12
13	34/14/M	Left	Occipito-temporal	Cryptogenic	Left temporoparietal	Left inferior occipito-temporal	–	–	–
14	15/0/F	Left	Parieto-temporal	Tuberous sclerosis	Left temporal	+	Left parietotemporal tuber	Ia	>12
15	46/3/F	Left	Temporal	HS	Left temporal	–	Left ATLR	Ia	3
16	13/10/M	Left	Temporal	Medial temporal DNT	Right temporal	–	Left ATLR	Ia	12
17	17/4/F	Left	Temporal	Medial temporal tumour	Left temporal	–	Lesionectomy	Ib	>12
18	5/2/F	Right	Temporal	Lateral temporal FCD	Right temporal	–	Lesionectomy	Ib	>12
19	15/10/F	Right	Temporal	Uncal dysplasia	Right temporal	–	Right ATLR	Ia	>12
20	38/32/F	Right	Temporal	HS	Right temporal	–	Right ATLR	Ib	>12
21	37/20/F	Right	Temporal	HS	Bilateral temporal	+	Right ATLR	Ia	>12
22	44/8/M	Right	Temporal	Hypothalamic haematoma	Right temporal	Right medial temporal	Right ATLR pending	–	–
23	30/19/M	Right	Temporal	HS	Right temporal	–	Right ATLR	Ia	12
24	28/20/F	Left	Temporal	HS	Left temporal	Left lateral temporal	–	–	–
25	25/11/F	Left	Parietal	FCD	Left parieto-temporal	+	Left Parietal	Ia	>12

ATLR = anterior temporal lobe resection; DNT = dysembryoplastic neuro-epithelial tumour; FCD = focal cortical dysplasia; HS = hippocampal sclerosis; Ia = Seizure-free, no residual aura; Ib = Seizure-free, residual aura; icEEG = intracranial EEG; M/F = male/female.

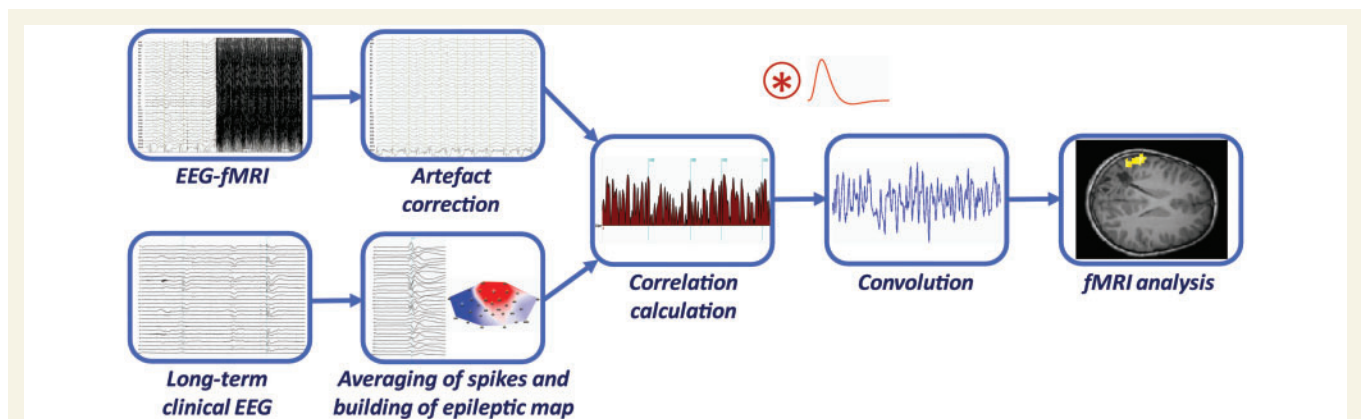


Figure 1 Schematic diagram of the topographic map correlation procedure. The EEG recorded in the scanner is corrected for artefacts (*top left*). Typical spikes derived from long-term EEG are averaged to build the epilepsy-specific EEG map (epileptic map *bottom left*). The time course of the correlation of this map with the intra-scanner EEG is calculated and this result is then convolved with the haemodynamic response function to build a regressor for functional MRI (fMRI) analysis.

for further analysis. After band-pass filtering (1–30 Hz using a second-order Butterworth filter), spikes were averaged and the EEG voltage map corresponding to the peak of the global field power of the average spike was considered as the epileptic map (Michel *et al.*, 2004a). The global field power corresponds to the spatial standard deviation and is defined as the sum of the squared potential

differences between all possible electrode pairs (Lehmann and Skrandies, 1980, 1984):

$$\text{GFP} = \sqrt{\sum_{i=1}^N \frac{(u_i - \bar{u})^2}{N}}$$

where u_i is the voltage at the electrode i , \bar{u} is the average voltage of all electrodes and N is the number of electrodes.

This measure quantifies the strength of a scalp potential field. The peak of the global field power was chosen to maximize the signal-to-noise ratio and the quality of the map.

The corrected intra-MRI EEG was first transformed into the electrode system of the long-term EEG using spline interpolation (Perrin *et al.*, 1987, 1989). Channels with artefact-ridden signal were excluded from this interpolation to improve data quality. EEG was then band-pass filtered between 1 and 30 Hz using a second-order Butterworth filter.

The presence of the epileptic map in the corrected intra-MRI EEG was quantified by means of correlation-based fitting (Murray *et al.*, 2008). For each time frame of the intra-MRI EEG, we calculated the spatial correlation with the epileptic map template. Correlation is based only on topographic comparison by dividing the maps by the global field power with no consideration of the polarity (the absolute value of the correlation is used). The correlation is thus a pure measure of global topographic similarity (Koenig and Gianotti, 2009).

The time course of the square of the correlation coefficient quantifying the presence of the epileptic map was convolved with the canonical haemodynamic response function and used as a regressor for the functional MRI analysis. The square of the correlation coefficient was chosen in order to increase the 'weight' of the high correlation values compared with low values.

Spike-based (conventional) analysis

An experienced neurophysiologist (S.V.) manually searched for each type of intra-MRI spikes for each patient. Spikes were modelled as zero-duration events, convolved with a standard haemodynamic response function and used as a regressor for the functional MRI analysis.

Functional magnetic resonance imaging analysis

Preprocessing

Standard functional MRI preprocessing was performed using the SPM8 software (Wellcome Department of Imaging Neurosciences, University College London, <http://www.fil.ion.ucl.ac.uk/spm>). Spatial preprocessing of functional images included: (i) motion correction using rigid-body transformation; (ii) spatial smoothing with an isotropic Gaussian kernel of 4 mm full width at half-maximum; and (iii) co-registration of pre- and/or postoperative 3D T₁-weighted structural MRI with functional images using six-parameter rigid body co-registration (Ashburner and Friston, 1997).

Statistical analysis

Functional MRI time-series were analysed with a general linear model as implemented in SPM8 software (Wellcome Department of Imaging Neurosciences, University College London, <http://www.fil.ion.ucl.ac.uk/spm>). The regressor derived from the topographical or the conventional analysis was introduced as the effect of interest and the six motion-related parameters derived from the functional MRI re-alignment were included in the general linear model as covariates. In each patient, paired *t*-tests (SPM *t*-tests) were applied at each voxel to test for BOLD increases or decreases associated with the fitting regressor (or with the timing of the spikes in the validation group). The significance level was set to $P < 0.05$ corrected for multiple comparisons across the whole brain using FWE correction. In addition, maps were created at a significance level $P < 0.001$ uncorrected for multiple comparisons. In these uncorrected maps, we used a five

voxels extent threshold to discard BOLD changes occurring only in scattered voxels.

Evaluation of concordance with intracranial electroencephalography and resection area

In patients who were seizure-free following surgery, we defined the target area as the resection area and its immediate proximity (< 15 mm from resection margins and within the same sublobar cortical region). When intracranial EEG recordings were available, the target area was similarly defined as the immediate proximity from the electrodes involved in seizure onset (< 15 mm from electrode and within the same sublobar cortical region). This distance allows for the fact that neuroelectrical activity and the related haemodynamic changes do not perfectly match (Disbrow *et al.*, 2000). Results were classified in three groups according to the statistical significance of BOLD changes and their concordance with the validation methods: (i) concordant (+ +): any corrected BOLD cluster ($P < 0.05$ FWE correction) or the uncorrected BOLD cluster with statistical maximum ($P < 0.001$ uncorrected, five voxels extent threshold) located within the target area; (ii) moderately concordant (+): a non-maximal uncorrected BOLD cluster in the target area ($P < 0.001$ uncorrected, five voxels extent threshold); and (iii) discordant (–): absence of significant BOLD changes in the target area or diffuse bilateral BOLD changes (corrected or uncorrected, with thresholds as above). Moreover, in the validation group, the spatial distribution of spike-related and topography-related BOLD changes were compared.

Results

In patients with a large number of spikes, a review of typically 5–10 min of long-term EEG was sufficient to select typical spikes of the patient and build the epileptic map. In patients with no or few spikes during EEG–functional MRI, we reviewed an average of 67 min (range: 6–209 min) of long-term EEG to obtain epileptic maps built from an average of 38 spikes (range: 9–61). No additional spike was detected by a *posteriori* review of the EEG, notably at time points corresponding to high correlation. Sustained increases (> 200 ms) in the correlation coefficient (and therefore the main contribution to the convolved regressor) found in some patients were in most instances related to pathological focal slow activity at the epileptic focus with similar topography as the spikes. No other stereotyped EEG pattern could be detected by a *posteriori* review of time points of increases in the correlation coefficient that were not sustained.

Figure 2 illustrates the correlation coefficient time course during spike-and-wave discharges as well as comparison between the convolved correlation coefficient and spike conventional regressors. Figure 3 shows the EEG correlates of high values of the correlation coefficient in a patient with no spike-related BOLD changes.

Validation group

The results of conventional spike-related analysis applied in the validation group during simultaneous functional MRI recording are given in Table 3 (median number of intra-MRI spikes: 81,

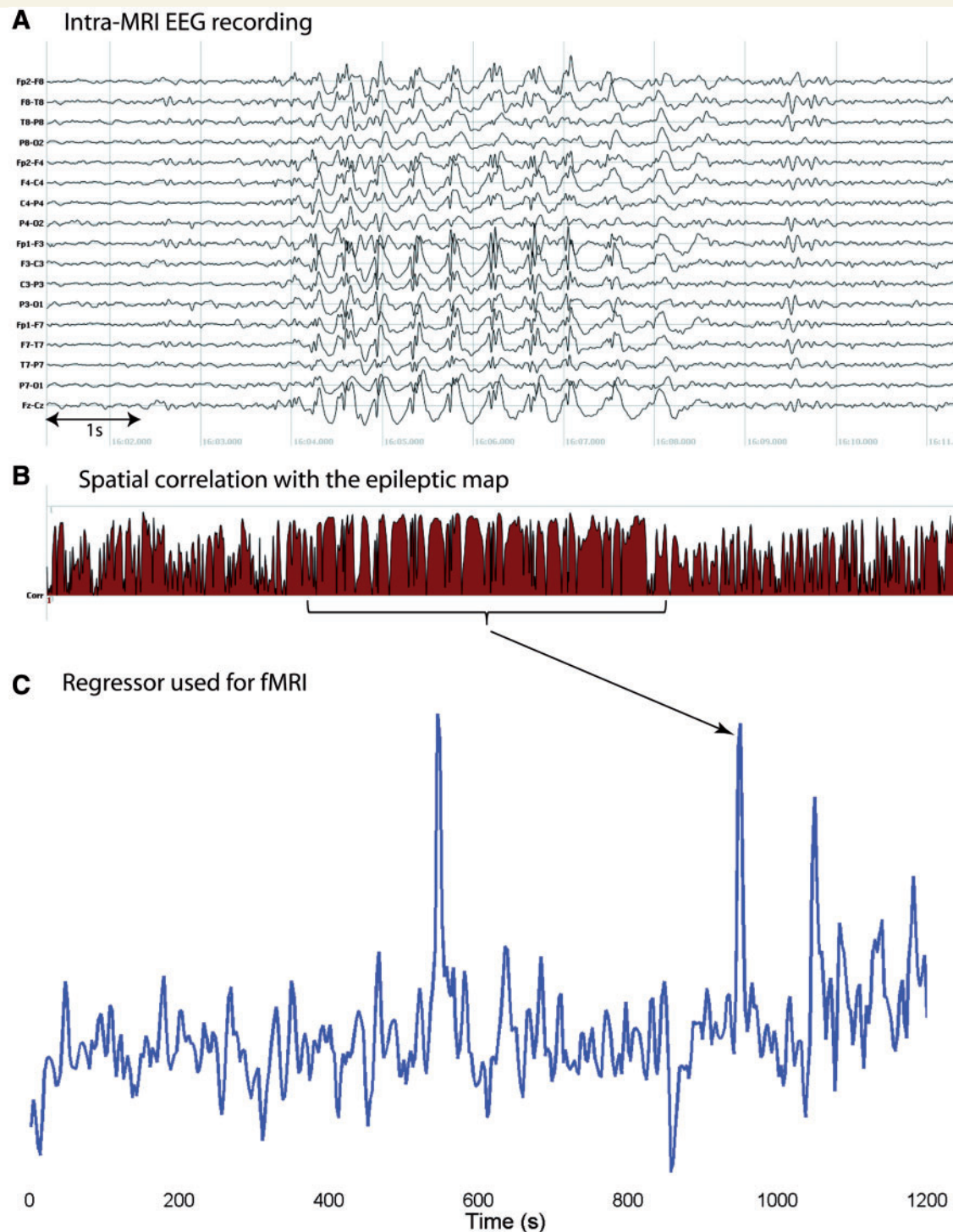


Figure 2 EEG and correlation coefficient in a patient with intra-MRI spikes (Patient 2). (A) Run of spikes in the intra-MRI EEG; (B) correlation coefficient for the same EEG segment: note the sustained duration of high correlation due to spikes and slow-wave who have similar topography (map polarity is not considered in the correlation); (C) functional MRI (fMRI) regressor obtained after convolution with the haemodynamic response function. Peaks in the regressor are related to sustained runs of spikes, as indicated by the arrow.

range: 30–1407). These spike-related BOLD changes (BOLD increases in 3/5, BOLD decreases in 2/5) were spatially concordant with the electroclinical evaluation in all five patients. In 4/5, the localization was further validated by intracranial EEG and/or

postoperative seizure freedom. Using the topography-based method, all of these patients showed significant topography-related BOLD changes surviving FWE correction and these were concordant with the results of conventional analysis and the

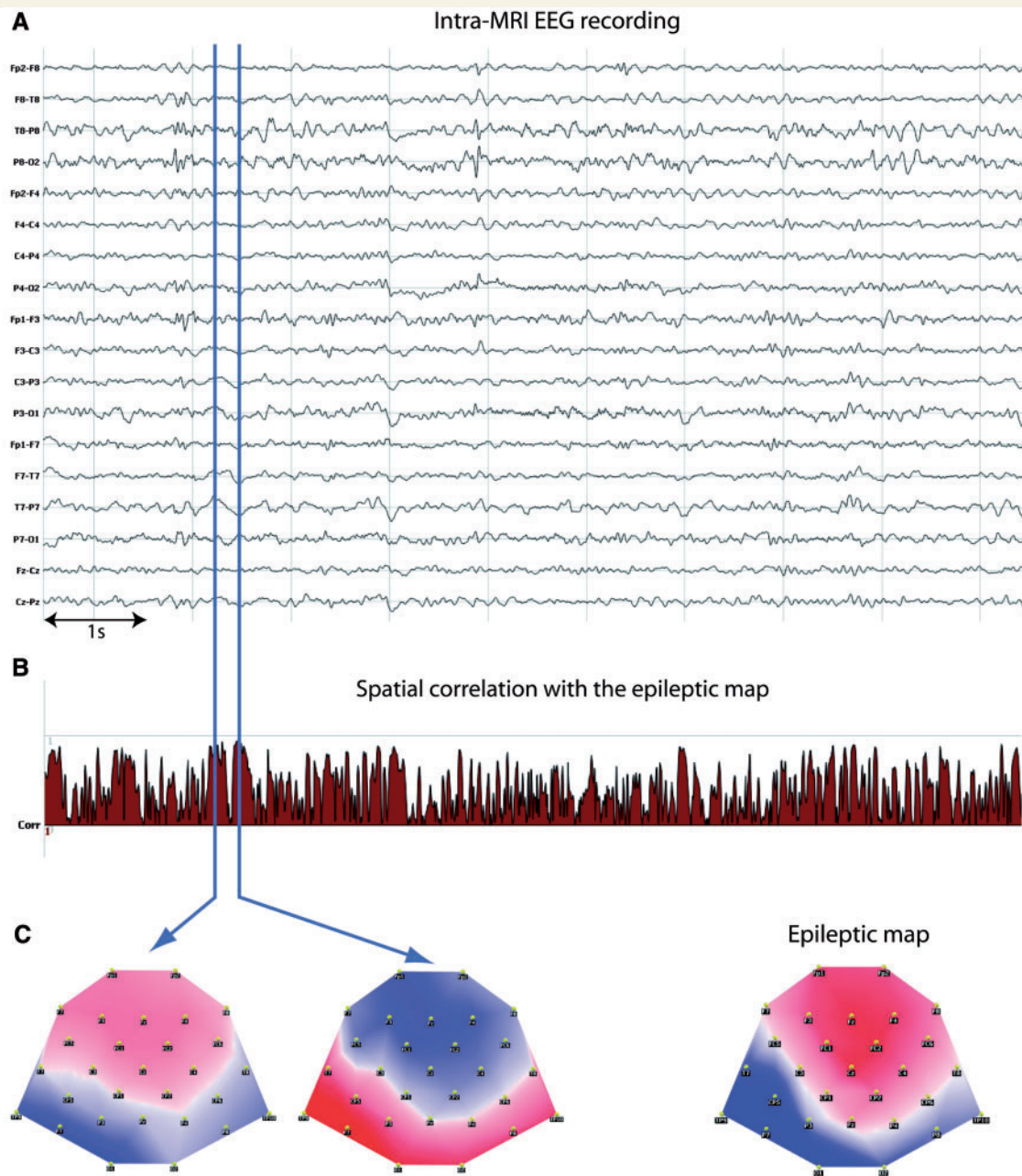


Figure 3 EEG and correlation coefficient in a patient without intra-MRI spikes (Patient 13). (A) Sample of intra-MRI EEG; (B) correlation coefficient for the same EEG segment. Blue vertical lines show time points with high correlation values. (C) The EEG maps (bottom left and centre) at these time points are highly correlated (or anti-correlated) with the epileptic map (bottom right). A posteriori review of the EEG revealed focal slow activity in the left temporal region simultaneous to the sustained increases of the correlation coefficient (T3–T5).

validation by intracranial EEG and/or surgical resection. (average correlation coefficient across time: range: 0.23–0.42, grand mean 0.35; standard deviation of the correlation coefficient: range: 0.16–0.24, grand mean 0.22).

This concordance is illustrated for Patient 1 in Fig. 4. This patient had suffered from tuberous sclerosis with two large tubers in left anterior frontal and left inferior frontocentral regions. Intracranial EEG recording showed spikes over the inferior frontocentral tuber with occasional concomitant involvement of the inferior frontal tuber. Seizure onset occurred independently in both

tubers. These were subsequently resected and the patient was seizure free 12 months after surgery. Both conventional and topographical analysis showed BOLD changes in the resection area of both tubers (statistical maximum in the left anterior frontal tuber).

Patients with inconclusive conventional analysis

Eighteen out of 20 patients with previously inconclusive EEG–functional MRI analysis were suitable for topographical analysis.

Table 3 Validation group: topography-related and spike-related BOLD changes

Patients	Topography-related BOLD increase			Spike-related BOLD increase			Topography-related BOLD decrease			Spike-related BOLD decrease		
	In target area	Max. in target area	Remote	In target area	Max. in target area	Remote	In target area	Max. in target area	Remote	In target area	Max. in target area	Remote
1	Left anterior frontal + left inferior frontal (FWE)	Yes	Left medial frontal, right cerebellum (FWE)	Left anterior frontal + left inferior frontal (in both resected tubers) (FWE) Left superior frontal (FWE)	—	Left medial frontal, Left thalamus (FWE)	—	—	Bilateral parietal + frontal right (unc.)	—	—	Bilateral parietal, frontal right (unc.)
2	Left superior frontal (FWE)	Yes	Left medial fronto-parietal, bilateral temporal (FWE)	Left superior frontal (FWE)	Yes	Left medial frontal (FWE)	—	—	bilateral parieto-temporal, head Left caudate (FWE) Basal ganglia (FWE)	—	—	Bilateral parieto-temporal (unc.)
3	Left parietal (FWE)	—	bilateral cingulate, Right temporal, Right cerebellum (FWE)	—	—	—	Left frontoparietal (FWE)	Yes	Basal ganglia (FWE)	Left frontoparietal (FWE)	Yes	Basal ganglia (FWE)
4	—	—	—	—	—	—	Right occipital (FWE)	—	Left temporal (FWE)	Right occipital (FWE)	Yes	—
5	Left parieto-occipital (FWE)	—	Left cerebellum, basal ganglia (FWE)	Left parieto-occipital (unc)	Yes	Left cerebellum, basal ganglia (unc.)	—	—	bilateral orbito-frontal, right parietal (FWE)	—	—	—

unc = uncorrected.

We found concordant and clinically meaningful results in 78% (14/18) of the patients. Topography-related BOLD changes were concordant (+ +) with the target area in 10, moderately concordant (+) in four and discordant (–) in four patients (average correlation coefficient across time: range: 0.22–0.48, grand mean: 0.37; standard deviation of the correlation coefficient: range: 0.16–0.26, grand mean: 0.22). Results were concordant or moderately concordant in 6/10 (60%) patients with medial/polar temporal lobe epilepsy and 8/8 (100%) patients with lateral temporal or extratemporal neocortical epilepsy, including temporal, frontal, parietal and occipital lobes. Two of the 20 patients (Patients 6 and 10) were excluded from further analysis due to excessive and repetitive head motion during EEG–functional MRI recordings (inter-scan motion >5 mm). Detailed localization of the BOLD clusters in individual patients is shown in Table 4.

Patients with good concordance (+ +)

We found concordant topography-related BOLD changes in 10 patients.

Patient 7 suffered from epilepsy symptomatic of a left prefrontal focal cortical dysplasia, BOLD changes were concordant with the lesion and the sublobar resection that led to seizure freedom at 1 year follow-up (Fig. 5).

Patient 9 had left frontal lobe epilepsy symptomatic of a small area of focal cortical dysplasia. The analysis revealed BOLD changes related to the epileptic map concordant with the lesion, and with the subsequent intracranial EEG and tailored small resection. This patient was seizure free 1 year postoperatively.

Patient 11 had left parieto-occipital epilepsy following neonatal bacterial meningoencephalitis with resultant gliosis. The area of maximal BOLD decrease was found within the area of gliosis, concordant with intracranial EEG.

Patient 12 suffered from right medial post-central epilepsy caused by a focal cortical dysplasia. The statistical maximum of the BOLD changes was concordant with the intracranial EEG and the small resection. She was seizure free 1 year after tailored corticectomy.

Patient 13 had cryptogenic left temporo-occipital epilepsy and the BOLD changes were highly concordant with the seizure onset zone and irritative zone determined by subdural grid recording. The patient declined the resection owing to the risk of a visual field defect (Fig. 6).

Patient 14 had tuberous sclerosis and a left parieto-temporal epileptic tuber identified by intracranial EEG and was seizure free after resection of this tuber. BOLD changes concordant with the resection area were found.

In Patient 20, with right temporal lobe epilepsy and hippocampal sclerosis who was seizure free 12 months after surgery, concordant BOLD changes were found in the right temporal pole (Fig. 7).

Patient 21 suffered from right temporal lobe epilepsy with hippocampal sclerosis confirmed by intracranial EEG. Clusters of right hippocampal and temporal polar BOLD changes were concordant with the anterior temporal lobe resection that produced seizure freedom (12 months follow-up).

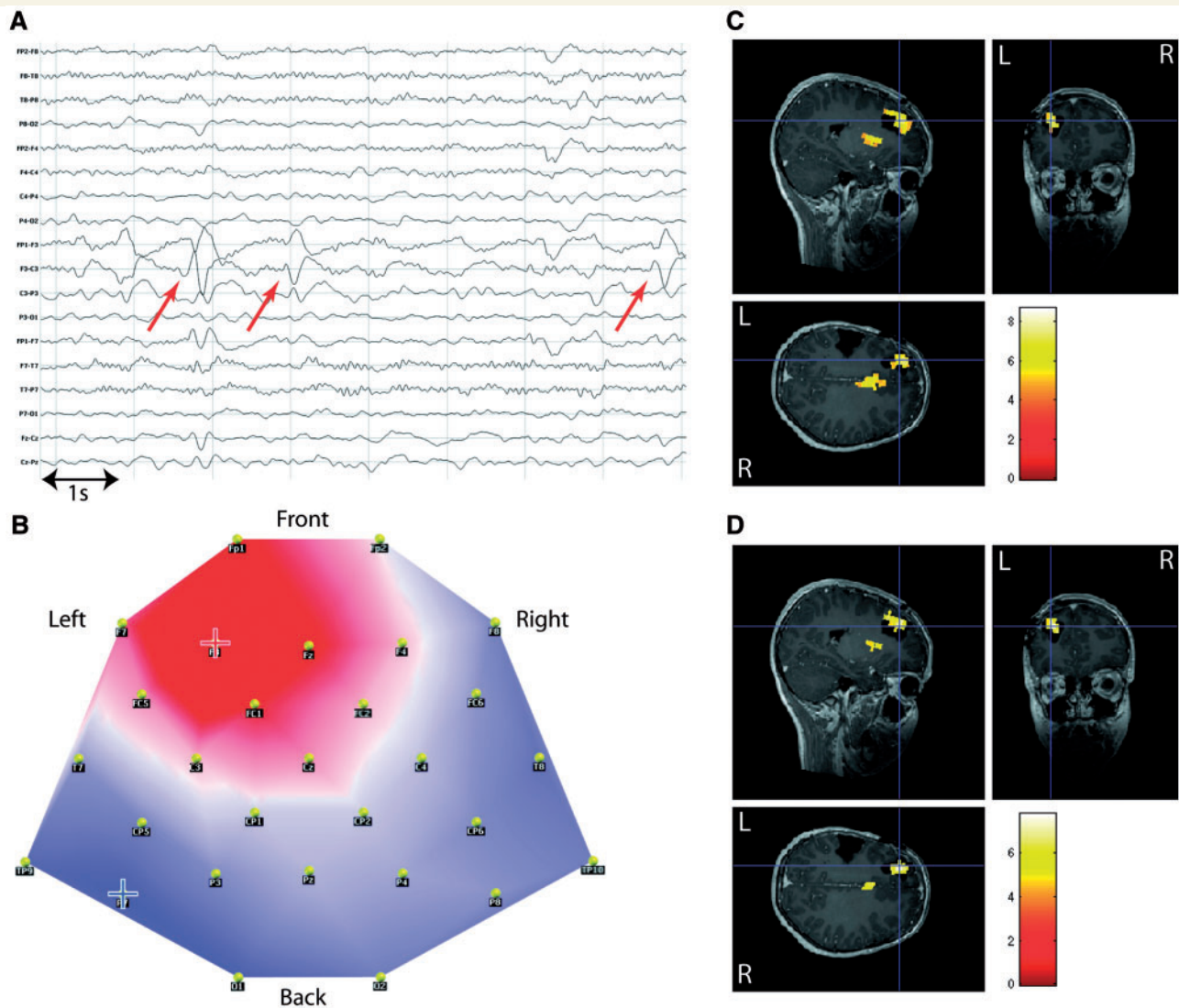


Figure 4 Validation of the topography-based analysis in a patient with spike-related BOLD changes. Patient 1, with left frontal epilepsy symptomatic of tuberous sclerosis: comparison of spike-related and topography-related BOLD changes. (A) Long-term EEG. Red arrow = representative spikes used to build epileptic map; (B) epileptic map derived from long-term EEG, blue/red cross indicates maximum negativity/positivity; (C) spike-related BOLD changes ($P < 0.05$, FWE correction); (D) topography-related BOLD changes ($P < 0.05$, FWE correction); C and D are co-registered with postoperative T₁-weighted MRI (resection of two tubers: left anterior frontal and inferior frontal).

Patient 24 had left temporal lobe epilepsy with hippocampal sclerosis and underwent intracranial EEG because of atypical scalp spikes. The irritative zone included left hippocampus and lateral temporal neocortex and the seizure onset was localized in the lateral temporal lobe with rapid propagation to the atrophic hippocampus. The maximal BOLD increase was in the right hippocampus, concordant with both the intracranial irritative and seizure onset zones.

Patient 25 had very frequent spikes during functional MRI acquisition but conventional EEG–functional MRI analysis failed to reveal significant BOLD changes. She had left parietal epilepsy due to a focal cortical dysplasia. Following intracranial EEG, she underwent tailored corticectomy and has been seizure free for 12

months. The topography-based analysis revealed a maximal BOLD increase concordant with the resection.

Patients with moderate concordance (+)

Moderately concordant topography-related BOLD changes were obtained in four patients.

Patient 8 had post-traumatic left frontal lobe epilepsy. BOLD decrease was found in the immediate vicinity of the cortical resection (tailored by intracranial EEG), which led to seizure freedom at 12 months follow-up.

Patient 16 had a left medial temporal dysembryoplastic neuro-epithelial tumour. The patient was seizure free 1 year after surgical

Table 4 Topography-related BOLD changes in patients without previously inconclusive EEG–functional MRI

Patients	Spikes in scanner	Topography-related BOLD increase			Topography-related BOLD decrease			Concordance with icEEG/resection			
		In target area	Max. in target area	Remote	In target area	Max. in target area	Remote				
		Number of clusters		Number of clusters		Number of clusters					
		FWE	unc.	FWE	unc.	FWE	unc.				
Patients without (or <10) spikes during EEG–functional MRI											
7	8	Left frontal (FWE)	Yes	Right frontal (FWE)	3 (0)	9	–	Bilateral parietal and occipital (FWE)	3 (0)	9	++
8	0	–	–	Cerebellum (unc.)	–	15	Left fronto-central (unc.)	Bilateral frontal (FWE)	6 (0)	28	+
9	0	Left superior frontal (FWE)	Yes	Bilateral inferior frontal (FWE)	5 (0)	2	–	Bilateral opercular, bilateral medial parietal (FWE)	24 (7)	26	++
11	0	–	–	Left anterior temporal, Left parieto-occipital (FWE)	7 (1)	21	Left parietal (FWE)	Right parietal, bilateral prefrontal (FWE)	10 (3)	19	++
12	9	Right parietal (unc)	Yes	Left inferior frontal, left parietal, left basal ganglia (unc.)	–	6	–	–	–	–	++
13	0	Left temporo-occipital (FWE)	Yes	Bilateral hippocampus, cingulate (FWE)	35 (7)	13	–	Left occipitotemporal (FWE)	5 (1)	6	++
14	0	Left parietal (FWE)	Yes	–	4 (1)	1	–	Left frontal superior (unc.)	–	2	++
15	4	Diffuse bilateral (FWE)	–	–	71 (18)	8	–	Scattered bilateral superior frontal (FWE)	5 (0)	3	–
16	2	Left hippocampus (unc)	–	Right thalamus (unc.)	–	4	Diffuse bilateral (FWE)	–	59 (14)	20	+
17	0	–	–	Left medial parietal (unc.)	–	1	–	Bilateral central gyrus, bilateral parietal, bilateral prefrontal (FWE)	12 (4)	19	–
18	1	–	–	–	–	–	–	Right posterior temporal, left occipital, bilateral cingulate, left frontal (unc.)	1 (0)	7	–
19	5	–	–	Bilateral opercular, right medial parietal (FWE)	9 (2)	13	–	Left temporo-occipital (unc.)	–	1	–
20	3	Right temporopolar (unc)	Yes	Left temporopolar (unc.)	–	2	–	Bilateral parietal, bilateral frontal (FWE)	8 (3)	9	++
21	4	Right temporopolar, right hippocampus (unc.)	Yes	Brainstem, bilateral cerebellum (unc.)	–	6	–	Bilateral medial and lateral frontal (unc.)	–	10	++
22	0	–	–	–	–	–	Right hippocampus (unc)	Bilateral occipital, left temporopolar (FWE)	9 (1)	18	+
23	0	Right temporopolar (unc.)	–	Bilateral opercular (FWE), medial parietal, left temporopolar, brainstem (unc.)	10 (4)	21	–	–	–	–	+
24	0	Left hippocampus, Left temporal basal (unc.)	Yes	Right hippocampus, bilateral prefrontal (unc.)	–	11	–	Medial parietal (unc.)	–	1	++
Patient with frequent spikes during EEG–functional MRI but absence of spike-related BOLD changes											
25	310	Left parietal (unc)	Yes	Left posterior frontal, bilateral occipital (unc.)	–	6	–	–	–	–	++

unc = uncorrected. For uncorrected results, clusters > 5 voxels are reported, whereas for FWE corrected results, the total number of clusters as well as the number of clusters > 5 voxels (between brackets) are reported.

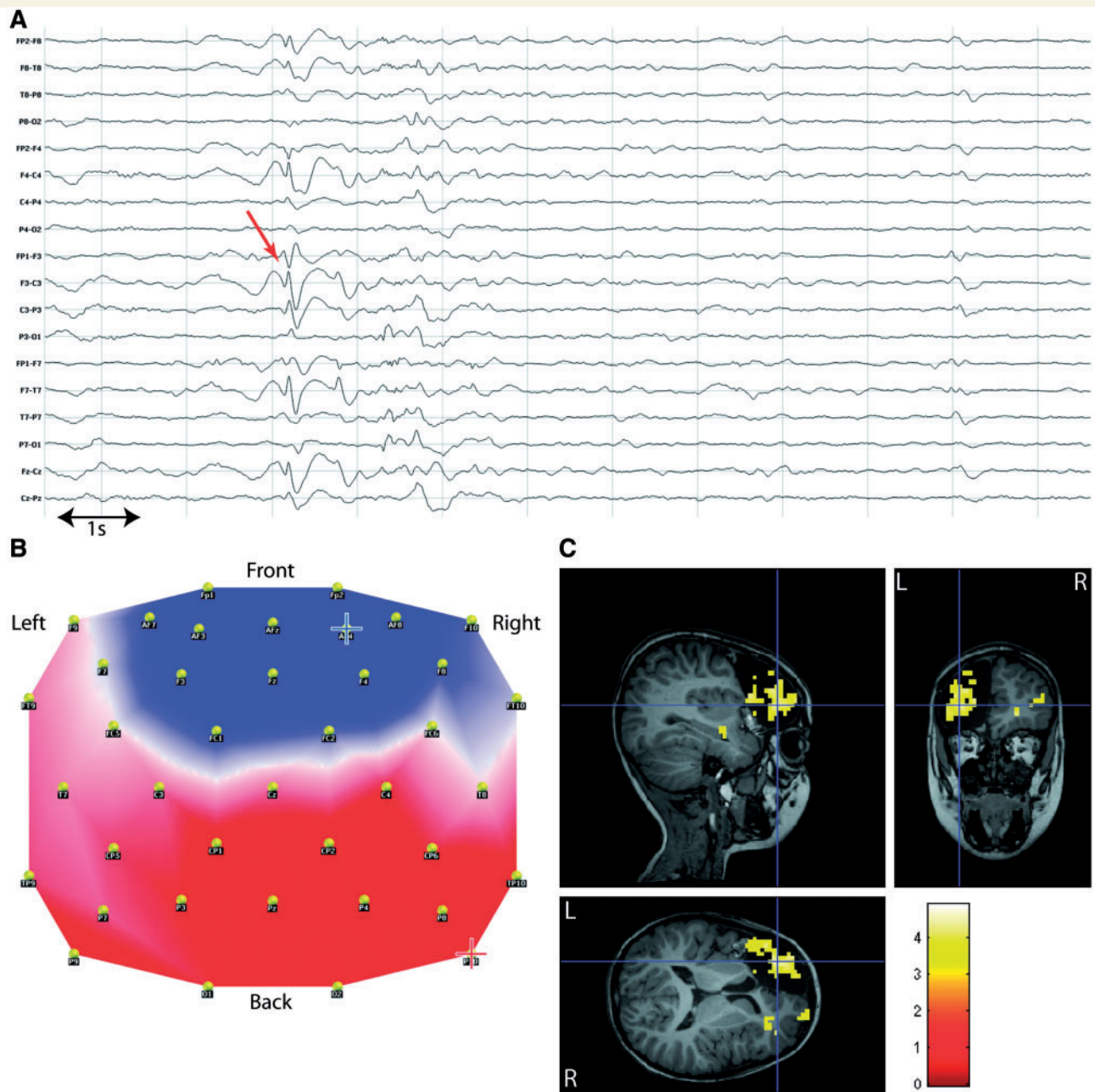


Figure 5 Concordant localization in frontal lobe epilepsy. Patient 7 with left frontal epilepsy, focal cortical dysplasia. (A) Long-term EEG. Red arrow = representative bilateral frontal spikes used to build the epileptic map; (B) epileptic map derived from long-term EEG, blue/red cross indicates maximum negativity/positivity (lateralization of the maximum negativity to the paramedian contralateral frontal lobe could be due to the inverted orientation of the medial frontal pyramidal neurons or to spike propagation resulting in a larger spike amplitude detected over the unaffected contralateral cortex); (C) topography-related BOLD changes ($P < 0.001$, uncorrected) co-registered with postoperative T₁-weighted MRI (12 months seizure free after left frontal lesionectomy).

resection and one of the four positive BOLD clusters was concordant with the resected region.

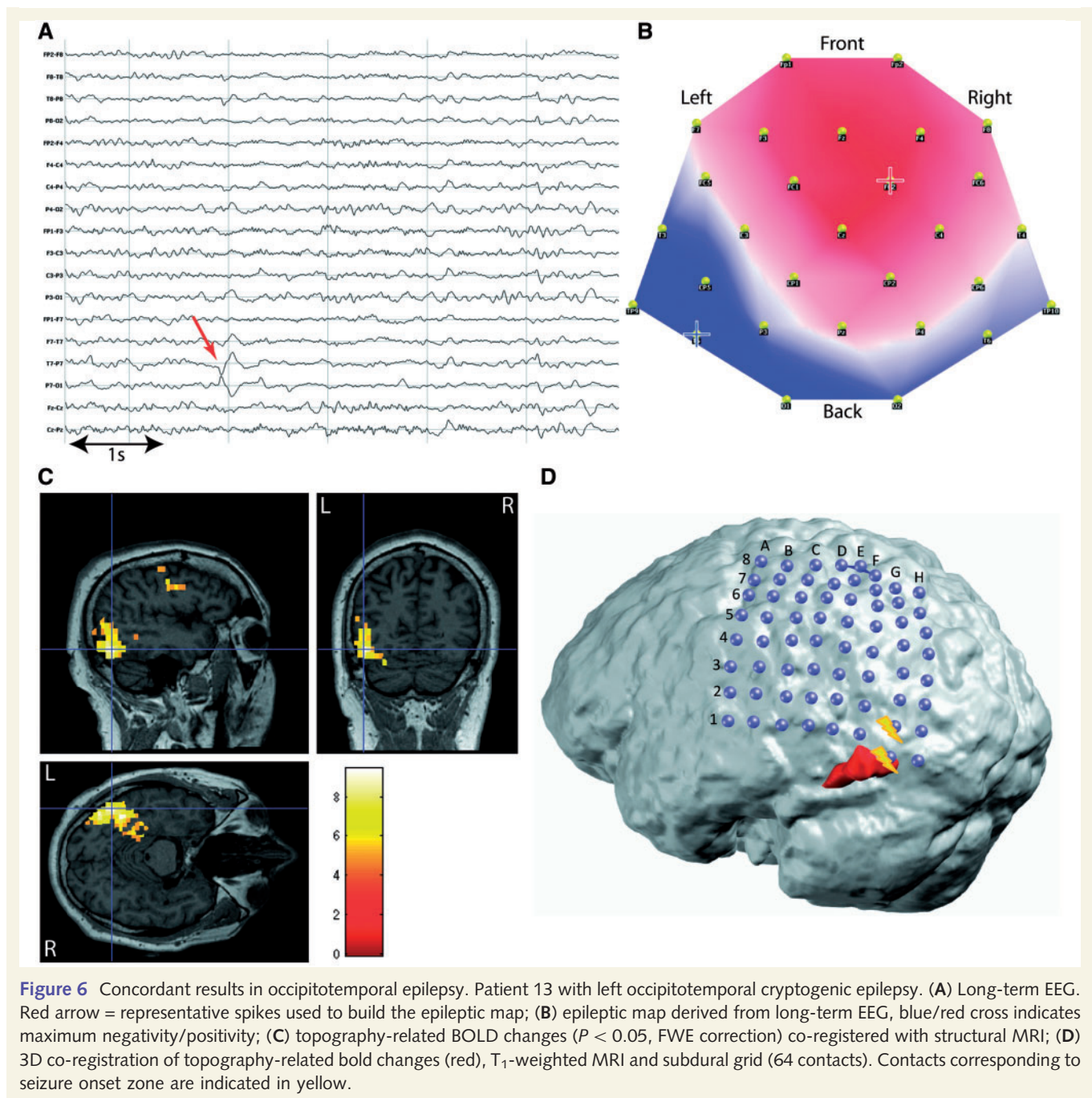
Patient 22 had right medial temporal lobe epilepsy confirmed on intracranial EEG. A region of concordant BOLD decrease was localized in the right hippocampus. He is awaiting surgery.

Patient 23 had right temporal lobe epilepsy with hippocampal sclerosis and has been seizure free for 12 months following anterior temporal lobe resection. Concordant BOLD changes were

found in the right temporal pole. We also found areas of BOLD increase remote from the target area in bilateral opercular regions and medial parietal cortex (see below).

Patients with discordant BOLD changes

There were discordant topography-related BOLD changes in four patients. All of these patients had medial/polar temporal lobe epilepsy. One had no clusters of BOLD increase (Patient 18) and one



had diffuse bilateral BOLD increase (Patient 15). In the latter, the diffuse bilateral BOLD increase strongly suggested contamination of EEG by artefact that could not be clearly identified (good quality of epileptic map, good quality of corrected intra-MRI EEG). In Patient 17, we found remote bilateral BOLD increase and decrease in the lateral frontal and lateral parietal lobes as well as the medial parietal regions. In Patient 19, we found areas of BOLD increase remote from the target area in bilateral opercular regions and medial parietal cortex in a pattern that was strongly suggestive of the auditory resting state network (Beckmann *et al.*, 2005; Mantini *et al.*, 2007) (Fig. 8). Such distant BOLD changes were

also found in Patient 23 where they co-existed with concordant BOLD changes.

Investigation of electroencephalography-related and other factors on the degree of concordance

High-quality scalp voltage maps of spikes and intra-MRI EEG were necessary to obtain concordant results and could be obtained using interpolation of artefact-affected electrodes and iterative artefact correction of the intra-MRI EEG. This was possible in all but two patients who were discarded. We found a higher proportion of good concordance in patients

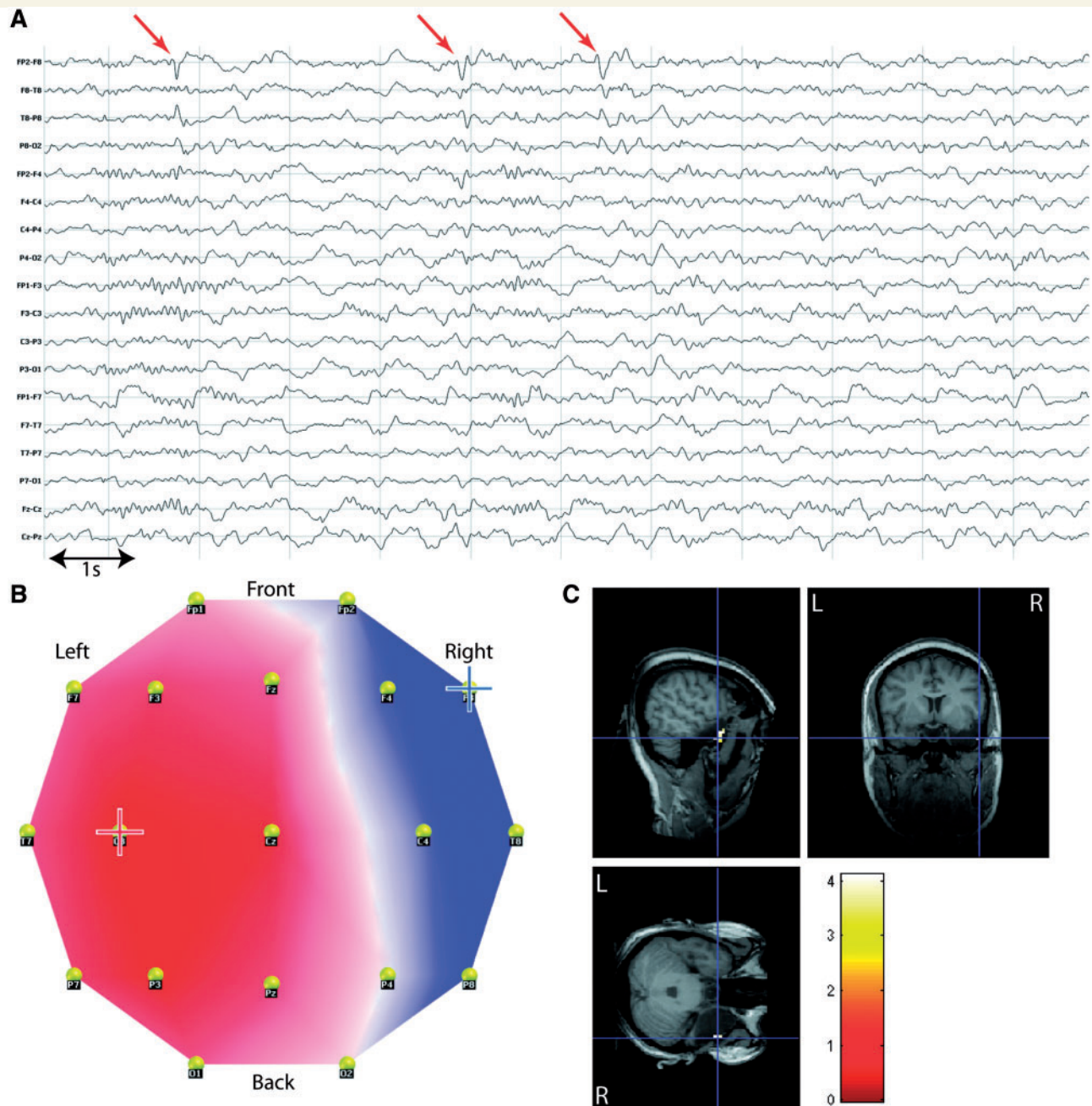


Figure 7 Concordant results in medial/polar temporal lobe epilepsy. Patient 20 with right temporal epilepsy, hippocampal sclerosis. (A) Long-term EEG. Red arrow = representative spikes used to build the epileptic map; (B) epileptic map derived from long-term EEG, blue/red cross indicates maximum negativity/positivity; (C) topography-related BOLD changes ($P < 0.05$, FWE correction) co-registered with postoperative structural MRI (right anterior temporal lobectomy).

with neocortical temporal lobe epilepsy compared with medial/polar temporal lobe epilepsy. Besides this difference based on localization, none of the parameters investigated on the long-term EEG, used to derive the epileptic map or on the intra-MRI EEG, could be identified as predictive of a concordant or discordant result. The quality of the epileptic map and the corrected intra-MRI EEG were visually of similar quality in discordant cases and all concordant groups. There was also no

effect of the arousal states (wakefulness versus light/deep non-REM sleep). Different arousal states in the clinical EEG or inside the scanner did not relate to poorer concordance. In children who were sedated for the procedure (Patients 7, 18 and 19), we found discordant results in the temporal cases and concordant results in the frontal lobe suggesting that the focus localization, rather than the use of sedation, influenced the level of concordance.

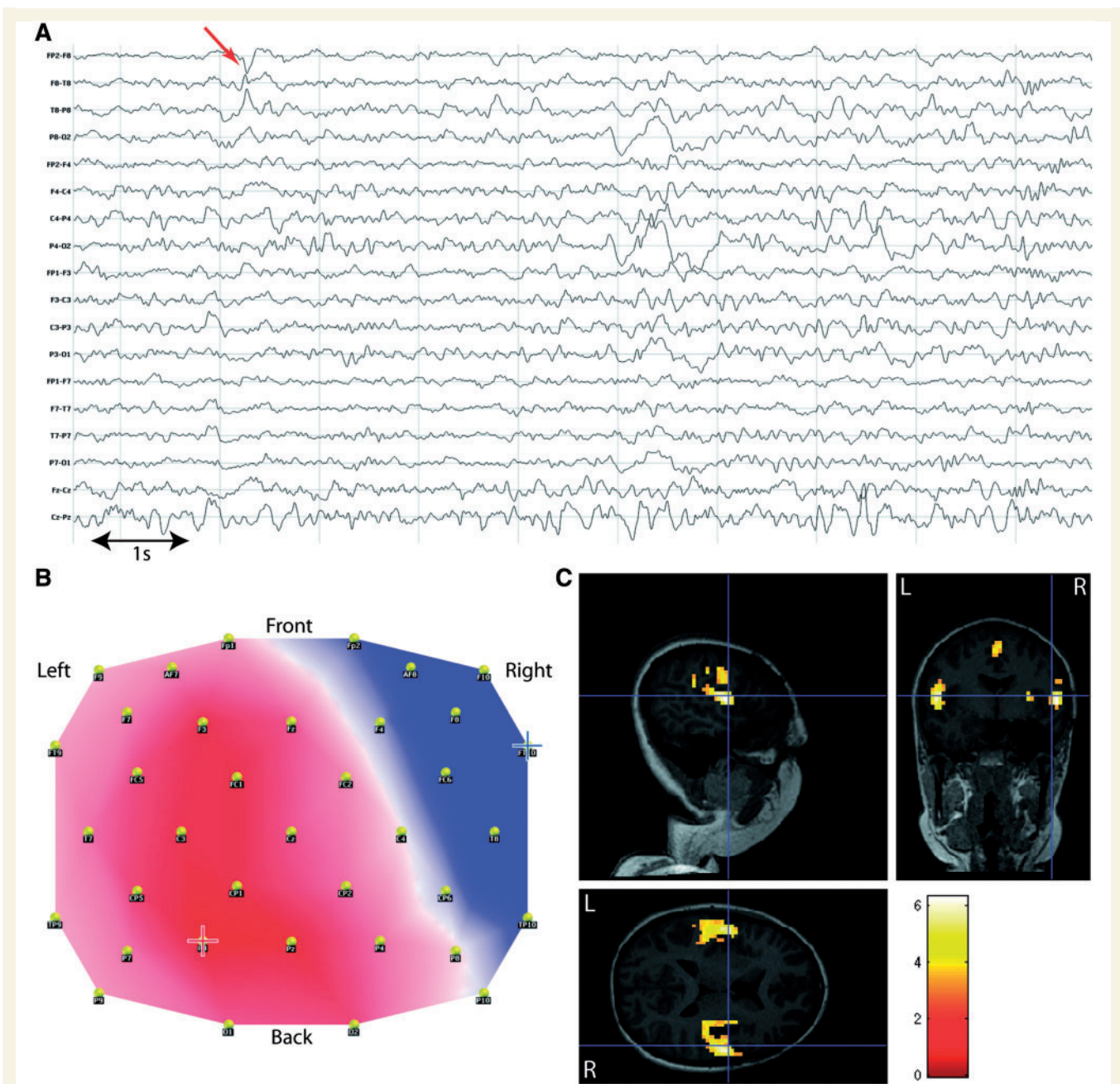


Figure 8 Discordant results in medial/polar temporal lobe epilepsy. Patient 19 with right temporal epilepsy, dysplasia of right uncus. (A) Long-term EEG. Red arrow = representative spikes used to build the epileptic map; (B) epileptic map derived from long-term EEG, blue/red cross indicates maximum negativity/positivity; (C) topography-related BOLD changes ($P < 0.001$, uncorrected for display but the bilateral opercular activations survived FWE correction, $P < 0.05$) co-registered with postoperative MRI (right anterior temporal lobectomy).

Discussion

EEG-derived voltage maps reflect the sum of the activity of the electrical sources in the brain at a given time and are a reliable marker of whole-brain activity. Our study represents the first evidence of haemodynamic correlates of EEG maps describing pathological brain activity. This further highlights the capacity of combined EEG–functional MRI to reveal focal epileptic activity not seen on conventional EEG.

In patients with focal epilepsy who are considered for surgery, concordant results of several localizing techniques are an important element for the planning of surgical resection or intracranial EEG electrode placement. We have shown that EEG–functional MRI combined with topographic information from routine clinical EEG could help localize focal epileptic activity in 78% of patients (100% in lateral temporal or extratemporal neocortical epilepsy and 60% in medial/polar temporal lobe epilepsy), in whom a previous conventional EEG–functional MRI analysis was negative,

suggesting this technique may provide novel information in these patients. In those with positive and concordant results using conventional analysis, the results of the new methodology were similarly concordant.

In addition, this is, to our knowledge, the largest EEG–functional MRI series in focal epilepsy with stringent validation of the results in all patients using intracranial EEG and/or surgical resection area.

Electroencephalography topographic maps: a marker of epileptic activity with haemodynamic correlates

Topography-based analysis of resting EEG in normal individuals typically reveals only a few stable maps (brain micro-states) that represent the instantaneous whole-brain electrical activity independent of frequency and are considered to be the building blocks of large-scale brain activity (Lehmann and Skrandies, 1980, 1984). In studies of pathological brain activity, EEG maps have long been shown to be a specific marker of epileptic activity (Ebersole and Wade, 1990; Lopes da Silva, 1990). Algorithms of inverse solutions applied to these maps reveal electrical sources formally corresponding to the irritative zone, which can be larger than the epileptogenic zone (Rosenow and Luders, 2001). For practical reasons, most non-invasive mapping techniques (EEG/MEG source imaging, EEG–functional MRI) map the irritative zone as a surrogate for the epileptogenic zone. Several studies have shown that the source of the spikes that is the most electroclinically relevant represents a good indicator of the epileptogenic zone (which includes the seizure onset zone), although some patients can show discordant results (Gavaret *et al.*, 2004; Ray *et al.*, 2007; Brodbeck *et al.*, 2009, 2010; Knowlton *et al.*, 2009; Thornton *et al.*, 2010a). Recent simultaneous EEG–functional MRI studies have shown that the physiological EEG maps have BOLD correlates corresponding to well-described resting state networks that fluctuate at radically different temporal scales (10 Hz versus 0.1 Hz) (Britz *et al.*, 2010). The existence of a relationship between these two measures of the resting brain activity is partly explained by the fact that the temporal sequence of EEG maps is scale invariant (Van De Ville *et al.*, 2010). In addition, the haemodynamic response to short-lasting events is characterized by BOLD changes stretching over several seconds (Glover, 1999). These considerations help understand the significant BOLD changes correlated with very short-lasting epilepsy related topographic maps found in our study.

Our hypothesis that, the occurrence of high correlation between the epileptic map and the resting EEG reflects increased activity of the epileptic generators was confirmed by the finding of correlated BOLD signal changes concordant with the seizure onset and/or epileptogenic zones. EEG maps seem, therefore, to be a sensitive and specific marker of focal activity related to the epileptic focus (spikes, focal slow waves) with associated BOLD signal changes in patients with and without intra-MRI spikes. Other increases in the correlation might be related to the occurrence of cortical spikes not identifiable as such on scalp recording, which represent the majority of epileptic activity recorded on the cortex (Alarcon *et al.*, 1994; Tao *et al.*, 2005). Simultaneous intracranial and scalp EEG

recordings with topographical scalp analysis would be needed to investigate this point but would be confounded by the current outflow caused by intracranial electrode implantation that distorts EEG topography.

In patients with medial/polar temporal lobe epilepsy, the degree of concordance was on the whole lower than for those with lateral temporal or extratemporal neocortical epilepsies. EEG maps showing frontal, parietal or occipital negativity are not found in healthy subjects and can be considered more specific of epileptic activity. However, the analysis of temporal lobe epilepsy cases with medial or polar epileptic focus is confounded by the similarity between EEG maps of temporal spikes and maps of physiological ‘resting’ brain activity. These physiological EEG maps correlate with BOLD signal changes seen in resting state networks (Britz *et al.*, 2010; Musso *et al.*, 2010). For example, in Patients 19 and 23 with temporal lobe epilepsy, the spatial pattern of remote BOLD increase related to the epileptic map showed some similarities with the auditory resting state network (Beckmann *et al.*, 2005; Mantini *et al.*, 2007), which has been shown to correlate with one of a small set of physiological topographical maps (Britz *et al.*, 2010; Musso *et al.*, 2010). Future studies including physiological EEG maps in the functional MRI analysis might help to disentangle such cases. The resting state-like BOLD changes are striking by their stereotypical and symmetrical spatial pattern and differed markedly from the lateralized BOLD changes found in the temporal lobe of concordant cases. This could help to avoid false localization of epileptic sources in these patients. Additional factors might contribute to the lower yield found in patients with temporal lobe epilepsy as reported in many EEG–functional MRI studies: the relative paucity of spikes in most awake patients with temporal lobe epilepsy and signal distortion and drop-out of echo-planar functional MRI in the inferior temporal regions due to the presence of bone and air in the underlying skull base (Bagshaw *et al.*, 2005, 2006; Salek-Haddadi *et al.*, 2006).

Maps of physiological and epileptic brain activity obtained from higher density EEG recordings (≥ 64 electrodes) or at least from EEG recordings including lower temporal electrodes, which could easily be added to long-term EEG recordings, might help to improve the specificity of the technique. So far, our technique requires consistent spikes to be identified on clinical recordings, but we hypothesize that clustering of EEG recordings (Michel *et al.*, 2004b) may allow identification of pathological epileptic maps and the use of this approach in patients with no or very sparse spikes on clinical recordings.

Comparison with other electroencephalography–functional magnetic resonance imaging methods in epilepsy

The conventional EEG–functional MRI analysis in epilepsy models the interictal spikes as events of ‘zero duration’ and constant amplitude that are used in an ‘event-related’ design for functional MRI analysis (Lemieux *et al.*, 2001; Salek-Haddadi *et al.*, 2006; Gotman, 2008). Prolonged discharges of spikes can be modelled as ‘blocks’ to enhance the statistical results (Bagshaw *et al.*, 2005; Salek-Haddadi *et al.*, 2006). Using these spike-related analysis

strategies, 40–70% of the EEG–functional MRI studies are inconclusive due to the lack of spikes during the functional MRI acquisition or absent significant BOLD correlation with the recorded spikes and this calls for alternative analysis strategies. The topography-based method has the potential advantage of capturing source strength variability and this may explain our positive findings in those patients with negative conventional EEG–functional MRI analysis despite a large number of spikes ('raised baseline' problem).

The use of functional MRI data-driven source identification has been proposed for EEG–functional MRI studies in which no spikes were detected during functional MRI recordings but specificity was likely to be low (Rodionov *et al.*, 2007). So far, such data-driven analysis based on spatial independent component analysis of functional MRI data has only been reported in patients with spikes and results were concordant with those obtained from EEG-informed functional MRI analysis (general linear models based on spikes or seizures) (Rodionov *et al.*, 2007; LeVan and Gotman, 2009; Thornton *et al.*, 2010b; Moeller *et al.*, 2011). Similarly, other methods have used continuously varying variables to model epileptic activity; continuous electrical source imaging (Vulliemoz *et al.*, 2009a) has been shown to increase the yield of EEG–functional MRI by ~20%. Another strategy is to decompose the intra-MRI EEG with independent component analysis to obtain epilepsy-specific EEG regressors (Jann *et al.*, 2008; Marques *et al.*, 2009). This approach increased the proportion of cases with clinically concordant BOLD changes but requires spikes or clear focal slowing to be recorded inside the magnetic resonance scanner for the selection of the epileptic components. Furthermore, validation was largely based on MRI lesions and non-invasive presurgical electroclinical findings. Our current approach uses the spatial correlation coefficient of the reference topography as a continuously varying parameter for functional MRI analysis. This parameter can be considered as a sort of spatial filter similar to the use of the strength of a dipolar source (Liston *et al.*, 2006) or the current density in a region of interest estimated by electrical source imaging (Vulliemoz *et al.*, 2009a). However, even when applied to patients who have spikes in the scanner (Vulliemoz *et al.*, 2009a), the results of using the map correlation as a regressor appear to be better than the local source strength. This is probably due to the fact that EEG maps of spikes reflect large-scale electrical brain activity rather than focal 'user-identified' activity. Moreover, EEG artefacts and noise are very unlikely to create EEG maps highly correlated to epilepsy-specific or physiological maps, but these artefacts can significantly alter the estimated source signal and confound the results of the source estimation techniques. Our results show that the map correlation coefficient can be used as a regressor in individuals with or without spikes recorded in the scanner and provided clinically meaningful results in most of the data sets that were thus far inconclusive.

Methodological considerations

Reliability of BOLD changes correlated with epileptic maps

Data from two patients (8%) were not suitable for analysis due to poor quality of EEG–functional MRI recordings related to motion,

electrode artefacts or difficulties in correcting MRI gradient- or pulse-related artefacts. The map correlation calculation and functional MRI analysis are user-independent resulting in a significant time saving and increased reliability in patients with spikes, especially those with very frequent or multi-focal spikes (Webber *et al.*, 1994). Variations in spike labelling can lead to significantly different results in spike-related EEG–functional MRI studies (Flanagan *et al.*, 2009), which may account for variations found in reproducibility studies (Salek-Haddadi *et al.*, 2006; Gholipour *et al.*, 2010).

We used EEG maps at the peak of the average spike as this provided better signal-to-noise ratios. However, the topographical map (and consecutive inverse solution) of the rising phase of the spikes has been reported to more accurately localize focal epileptic activity when compared with maps at the spike peak (Lantz *et al.*, 2003). Applying our method to EEG maps derived from the spike rising phase did not alter the BOLD patterns significantly, probably as a result of a fixed pattern of spike propagation.

Despite careful exploration of EEG features both on the clinical EEG and the intra-MRI recordings, we were not able to identify factors that would predict discordant results and might serve as criteria for patient selection. Besides the need for a very carefully constructed epileptic map and optimal quality of the corrected intra-MRI EEG (Grouiller *et al.*, 2007), the only factor associated with the presence of concordant results was the localization of the epileptic focus outside the medial/polar temporal lobe. Besides the argument of similarity between temporal lobe epilepsy maps and maps of physiological 'resting' brain activity discussed above, the low number of electrodes in the long-term EEG from which the epileptic maps were constructed probably also contributed to the worse result of the temporal lobe epilepsy cases. EEG source localization studies have shown the importance of lower temporal electrodes to correctly sample the electric field of temporal lobe epilepsy spikes (Sperli *et al.*, 2006). A higher number of electrodes in the long-term EEG are nowadays feasible and, together with high density recordings inside MRI scanners, will further increase the sensitivity of our method (Holmes *et al.*, 2010).

Validation

In patients with focal epilepsy, several validation strategies can be considered for novel neuroimaging techniques (Vulliemoz *et al.*, 2010): from spatial concordance with existing non-invasive data to more stringent validation with intracranial EEG recording or postoperative imaging of the resection area in patients who are seizure free [which can be considered an approximation of the epileptogenic zone: 'the tissue which, if resected, results in seizure freedom' (Rosenow and Luders, 2001)]. The best available gold standard is the combination of the epileptogenic zone identified on intracranial EEG and postoperative seizure freedom following its resection, although large series with adequate follow-up are very difficult to obtain with such strict criteria. Previous studies have shown concordance of EEG–functional MRI results with intracranial EEG (Benar *et al.*, 2006) or postoperative outcome (Thornton *et al.*, 2010a). Given these findings, we first validated our method non-invasively by comparison with the conventional spike-based analysis. We found very good concordance and stronger BOLD changes with our topography-based analysis suggesting increased sensitivity. In the patients with inconclusive conventional

EEG–functional MRI analysis, both intracranial EEG and postoperative seizure freedom were available in half. In the other patients, unambiguous localization revealed by intracranial EEG or postoperative seizure freedom following focal resection was considered a robust validation. In our intracranial EEG recordings, the seizure onset zone was co-localized with the maximum focus of the irritative zone (i.e. the brain region generating the most frequent spikes), and we assumed that this area corresponded to the generators of the representative scalp spike used to build the epileptic map.

Regarding specificity, it is important to keep in mind that EEG–functional MRI reveals a network characterized by several clusters of BOLD changes so that the technique is not expected to specifically pinpoint the source of epileptic activity. Nevertheless, in more than half of our patients (10/18), the localization of the statistical maximum was specifically concordant with the target area. The numbers of significant clusters provided in Table 4 provide some information regarding the intra-individual specificity of the cluster found to be concordant. However, such numbers can be misleading when several clusters are very close together, as these might represent a single neurophysiological 'area of interest', fragmented by small data smoothing kernels or strict statistical thresholds. We opted for a canonical haemodynamic response function as deviation from the canonical haemodynamic response function related to focal spikes is generally small (Lemieux *et al.*, 2008). Using a more flexible function could increase sensitivity but at the cost of specificity. In the discordant cases, subsequent analysis with a more flexible function (temporal and dispersion derivatives) did not yield more meaningful results.

Clinical implications

More than a decade after the first EEG–functional MRI results were validated with intracranial EEG (Seeck *et al.*, 1998), only a few studies have specifically investigated the reliability of the localization provided by EEG–functional MRI. Neuroelectrical activity and related haemodynamic changes of physiological and pathological brain function in animals and in humans do not show exact overlap and a concordance within 20 mm is generally accepted (Disbrow *et al.*, 2000; Benar *et al.*, 2006; Vulliemoz *et al.*, 2009b). Therefore, focal BOLD changes can act as a regional marker of epileptogenic networks at a macroscopic scale and this localizing information is a robust complementary tool in the planning of invasive EEG or resective surgery. Previous studies have confirmed the reproducibility of EEG–functional MRI findings (Salek-Haddadi *et al.*, 2006; Gholipour *et al.*, 2010). Rigorous validation of the localization with intracranial data was obtained in a few small series: Lazeyras *et al.* (2000) reported BOLD signal changes concordant with intracranial EEG in 5/6 patients. Comparing BOLD changes with the irritative zone measured by intracranial depth electrodes in five patients in separate sessions, Benar *et al.* (2006) found epileptiform activity in most contacts within 20–40 mm of the BOLD changes. In another study, Thornton *et al.* (2010a) found that focal BOLD changes restricted to the resection zone predicted postoperative seizure freedom. The study reviewed EEG–functional MRI studies of 76 patients where 21 patients (28%, none of them included in the

present study) showed significant BOLD changes and 10 of them were operated (seven seizure free).

In patients with no or very infrequent scalp spikes recorded in the scanner, EEG–functional MRI studies are usually considered inconclusive. BOLD correlates of focal slow EEG activity have been shown to be spatially concordant with the epileptogenic focus but only a minority of these cases had stringent validation of the findings (Lazeyras *et al.*, 2000; Jann *et al.*, 2008; Manganotti *et al.*, 2008; Grouiller *et al.*, 2010). Our method dramatically increased the yield of EEG–functional MRI studies in epilepsy irrespective of the presence or absence of spikes during functional MRI recording. At the same time, our study represents the largest EEG–functional MRI study in epilepsy with robust clinical validation (see below). This provides additional support for a potential role for EEG–functional MRI as a valuable localizing tool for the irritative zone provided detectable spikes are found on clinical recordings. At present, EEG–functional MRI could be used to guide implantation of intracranial electrodes to localize epileptic generators. Further studies comparing topography-related EEG–functional MRI results in patients with various postoperative outcomes will be needed to assess the predictive value of the method on postoperative outcome, as done recently for spike-related EEG–functional MRI (Zijlmans *et al.*, 2007; Thornton *et al.*, 2010a).

Since we used spike maps derived from clinical recordings, our method is applicable to any epilepsy centre where EEG–functional MRI is performed. Localizing BOLD changes related to epileptic activity can lead to a change in the clinical management (Zijlmans *et al.*, 2007; Moeller *et al.*, 2009) and using the topography-based method for retrospective analysis of previously recorded EEG–functional MRI without spike may provide clinically relevant information.

We found particularly good concordance in patients with neocortical epilepsy, notably frontal lobe epilepsy. Presurgical evaluation of patients with frontal lobe epilepsy is frequently complicated by poor localization of seizure onset on conventional EEG monitoring, often making intracranial EEG with extensive coverage necessary. Our study complements the previous findings in a minority of patients with frontal lobe epilepsy studied with conventional EEG–functional MRI analysis (Moeller *et al.*, 2009). The increased sensitivity obtained in our study provides strong evidence for a potential clinical role for EEG–functional MRI in these difficult presurgical cases.

We also found good concordance in patients with tuberous sclerosis. These patients with multiple lesions can often be improved by surgery but the identification of the most epileptogenic tuber(s) often requires intracranial EEG recordings. EEG–functional MRI maps appear to be a good marker of epileptogenicity to plan intracranial EEG and surgery in these patients (Jacobs *et al.*, 2008b). Our method extends the use of the technique to patients with a small number of spikes on EEG and offers increased EEG–functional MRI yield in this group.

We found non-maximal BOLD decrease in the target area in three patients. BOLD decreases related to interictal epileptic activity can have localizing value in some patients (Kobayashi *et al.*, 2006; Vulliemoz *et al.*, 2009a), especially in children (Jacobs *et al.*, 2007), although they are more frequently found remote from the

epileptogenic zone (Salek-Haddadi *et al.*, 2006). Moreover, negative BOLD changes close to spiking intracranial electrodes have been reported (Benar *et al.*, 2006). The underlying mechanisms responsible for the sign of BOLD signal changes in individual patients remain incompletely understood (Gotman, 2008). Changes in neuronal inhibition surrounding the epileptic focus could lead to a regional decrease in metabolic demand. In addition, concordant BOLD decreases are sometimes preceded by BOLD increases at the same location suggesting an altered haemodynamic response function (Jacobs *et al.*, 2009; Rathakrishnan *et al.*, 2010), while a local vascular steal mechanism seems less likely (Kobayashi *et al.*, 2006). An effect of age, vigilance, medication (sedation in some children) and spike frequency are also possible (Jacobs *et al.*, 2008a; Moehring *et al.*, 2008). In our five patients with spike-related BOLD changes, the sign of BOLD changes was congruent between the conventional analysis and the topography-related analysis suggesting that these hypotheses remain valid to explain the sign of topography-related BOLD changes. Therefore, we suggest that BOLD decrease should always be explored, especially in children or when regions of BOLD increase are discordant. Regions of remote BOLD decrease in our patients was often located in parts of resting state networks (Beckmann *et al.*, 2005), notably the default mode network (comprising bilaterally the precuneus, lateral temporo-parietal cortex and prefrontal cortex) (Gusnard *et al.*, 2001). BOLD decrease in the default mode network, especially the precuneus, has been associated with focal epileptic activity in the medial temporal lobe (Salek-Haddadi *et al.*, 2006; Laufs *et al.*, 2007; Kobayashi *et al.*, 2009) and with generalized epileptic activity (Gotman *et al.*, 2005; Hamandi *et al.*, 2008). These findings have been interpreted as reduced neuronal and metabolic activity in this network, most active during resting wakefulness, and linked with impaired awareness related to temporal lobe and generalized seizures.

Conclusion

We have described a novel method for the analysis of EEG–functional MRI data that reveals the correlation between epilepsy-specific EEG maps and BOLD changes validated against the gold standard for localization of focal epileptic activity. This can have significant implications in patients with focal epilepsy, with or without spikes recorded in the scanner, by increasing the yield of EEG–functional MRI studies and allowing localization of focal epileptic activity in the majority of patients with, to date, inconclusive EEG–functional MRI studies. We suggest that EEG–functional MRI could improve the presurgical evaluation of patients with medically refractory epilepsy, potentially increasing the number of patients for whom surgery is an option, and reducing surgical failures.

Acknowledgements

We are grateful to all our colleagues in the Radiology Departments and the Telemetry Wards at all three centres for their help in data collection.

Funding

The Cartool software has been programmed by D. Brunet, from the Functional Brain Mapping Laboratory, Geneva, Switzerland, and is supported by the Centre for Biomedical Imaging (CIBM) of Geneva and Lausanne. We are grateful to the Big Lottery fund, Wolfson Trust and The Epilepsy Society for supporting the Epilepsy Society MRI scanner. We acknowledge the financial support of the Swiss National Science Foundation (No. 33CM30-124089, 33CM30-124115 and 320030-122073); CIBM of Geneva and Lausanne. L.L. is supported by the UK Medical Research Council MRC grant G0301067 (with R.C.T.) and by Action Medical Research, the Brain Research Trust and the James Tudor Foundation. We also acknowledge the support of the Department of Health's NIHR Biomedical Research Centres funding scheme (University College London Hospital/University College London (UCLH/UCL), German Research Foundation (DFG grant SI 1419/2-1) and Sonderforschungsbereich SFB 855 (Subproject D3).

References

- Aghakhani Y, Kobayashi E, Bagshaw AP, Hawco C, Benar CG, Dubeau F, et al. Cortical and thalamic fMRI responses in partial epilepsy with focal and bilateral synchronous spikes. *Clin Neurophysiol* 2006; 117: 177–91.
- Alarcon G, Guy CN, Binnie CD, Walker SR, Elwes RD, Polkey CE. Intracerebral propagation of interictal activity in partial epilepsy: implications for source localisation. *J Neurol Neurosurg Psychiatry* 1994; 57: 435–49.
- Allen PJ, Josephs O, Turner R. A method for removing imaging artifact from continuous EEG recorded during functional MRI. *Neuroimage* 2000; 12: 230–9.
- Allen PJ, Polizzi G, Krakow K, Fish DR, Lemieux L. Identification of EEG events in the MR scanner: the problem of pulse artifact and a method for its subtraction. *Neuroimage* 1998; 8: 229–39.
- Ashburner J, Friston K. Multimodal image coregistration and partitioning—a unified framework. *Neuroimage* 1997; 6: 209–17.
- Bagshaw AP, Hawco C, Benar CG, Kobayashi E, Aghakhani Y, Dubeau F, et al. Analysis of the EEG–fMRI response to prolonged bursts of interictal epileptiform activity. *Neuroimage* 2005; 24: 1099–112.
- Bagshaw AP, Torab L, Kobayashi E, Hawco C, Dubeau F, Pike GB, et al. EEG–fMRI using z-shimming in patients with temporal lobe epilepsy. *J Magn Reson Imaging* 2006; 24: 1025–32.
- Beckmann CF, DeLuca M, Devlin JT, Smith SM. Investigations into resting-state connectivity using independent component analysis. *Philos Trans R Soc Lond B Biol Sci* 2005; 360: 1001–13.
- Bell AJ, Sejnowski TJ. An information-maximization approach to blind separation and blind deconvolution. *Neural Comput* 1995; 7: 1129–59.
- Benar CG, Grova C, Kobayashi E, Bagshaw AP, Aghakhani Y, Dubeau F, et al. EEG–fMRI of epileptic spikes: concordance with EEG source localization and intracranial EEG. *Neuroimage* 2006; 30: 1161–70.
- Britz J, Van De Ville D, Michel CM. BOLD correlates of EEG topography reveal rapid resting-state network dynamics. *Neuroimage* 2010; 52: 1162–70.
- Brodbeck V, Lascano AM, Spinelli L, Seeck M, Michel CM. Accuracy of EEG source imaging of epileptic spikes in patients with large brain lesions. *Clin Neurophysiol* 2009; 120: 679–85.
- Brodbeck V, Spinelli L, Lascano AM, Pollo C, Schaller K, Vargas MI, et al. Electrical source imaging for presurgical focus localization in epilepsy patients with normal MRI. *Epilepsia* 2010; 51: 583–91.

- Brunet D, Murray MM, Michel CM. Spatiotemporal Analysis of Multichannel EEG: CARTOOL. *Comput Intell Neurosci* 2011, doi:10.1155/2011/813870.
- Disbrow EA, Slutsky DA, Roberts TP, Krubitzer LA. Functional MRI at 1.5 tesla: a comparison of the blood oxygenation level-dependent signal and electrophysiology. *Proc Natl Acad Sci USA* 2000; 97: 9718–23.
- Duncan JS. Imaging in the surgical treatment of epilepsy. *Nat Rev Neurol* 2010; 6: 537–50.
- Ebersole JS, Wade PB. Spike voltage topography and equivalent dipole localization in complex partial epilepsy. *Brain Topogr* 1990; 3: 21–34.
- Engel JJ, Van Ness PC, Rasmussen TB. Outcome with respect to epileptic seizures. New York: Raven Press Ltd; 1993.
- Flanagan D, Abbott DF, Jackson GD. How wrong can we be? The effect of inaccurate mark-up of EEG/fMRI studies in epilepsy. *Clin Neurophysiol* 2009; 120: 1637–47.
- Gavaret M, Badier JM, Marquis P, Bartolomei F, Chauvel P. Electric source imaging in temporal lobe epilepsy. *J Clin Neurophysiol* 2004; 21: 267–82.
- Gholipour T, Moeller F, Pittau F, Dubeau F, Gotman J. Reproducibility of interictal EEG-fMRI results in patients with epilepsy. *Epilepsia* 2010; 52: 433–42.
- Glover GH. Deconvolution of impulse response in event-related BOLD fMRI. *Neuroimage* 1999; 9: 416–29.
- Gotman J. Epileptic networks studied with EEG-fMRI. *Epilepsia* 2008; 49 (Suppl 3): 42–51.
- Gotman J, Grova C, Bagshaw A, Kobayashi E, Aghakhani Y, Dubeau F. Generalized epileptic discharges show thalamocortical activation and suspension of the default state of the brain. *Proc Natl Acad Sci USA* 2005; 102: 15236–40.
- Groening K, Brodbeck V, Moeller F, Wolff S, van Baalen A, Michel CM, et al. Combination of EEG-fMRI and EEG source analysis improves interpretation of spike-associated activation networks in paediatric pharmacoresistant focal epilepsies. *Neuroimage* 2009; 46: 827–33.
- Grouiller F, Vercueil L, Krainik A, Segebarth C, Kahane P, David O. A comparative study of different artefact removal algorithms for EEG signals acquired during functional MRI. *Neuroimage* 2007; 38: 124–37.
- Grouiller F, Vercueil L, Krainik A, Segebarth C, Kahane P, David O. Characterization of the hemodynamic modes associated with interictal epileptic activity using a deformable model-based analysis of combined EEG and functional MRI recordings. *Hum Brain Mapp* 2010; 31: 1157–73.
- Gusnard DA, Akbudak E, Shulman GL, Raichle ME. Medial prefrontal cortex and self-referential mental activity: relation to a default mode of brain function. *Proc Natl Acad Sci USA* 2001; 98: 4259–64.
- Hamandi K, Laufs H, Noth U, Carmichael DW, Duncan JS, Lemieux L. BOLD and perfusion changes during epileptic generalised spike wave activity. *Neuroimage* 2008; 39: 608–18.
- Holmes MD, Tucker DM, Quiring JM, Hakimian S, Miller JW, Ojemann JG. Comparing noninvasive dense array and intracranial electroencephalography for localization of seizures. *Neurosurgery* 2010; 66: 354–62.
- Jacobs J, Hawco C, Kobayashi E, Boor R, Le Van P, Stephani U, et al. Variability of the hemodynamic response as a function of age and frequency of epileptic discharge in children with epilepsy. *Neuroimage* 2008a; 40: 601–14.
- Jacobs J, Kobayashi E, Boor R, Muhle H, Stephan W, Hawco C, et al. Hemodynamic responses to interictal epileptiform discharges in children with symptomatic epilepsy. *Epilepsia* 2007; 48: 2068–78.
- Jacobs J, Levan P, Moeller F, Boor R, Stephani U, Gotman J, et al. Hemodynamic changes preceding the interictal EEG spike in patients with focal epilepsy investigated using simultaneous EEG-fMRI. *Neuroimage* 2009; 45: 1220–31.
- Jacobs J, Rohr A, Moeller F, Boor R, Kobayashi E, Le Van Meng P, et al. Evaluation of epileptogenic networks in children with tuberous sclerosis complex using EEG-fMRI. *Epilepsia* 2008b; 49: 816–25.
- Jann K, Wiest R, Hauf M, Meyer K, Boesch C, Mathis J, et al. BOLD correlates of continuously fluctuating epileptic activity isolated by independent component analysis. *Neuroimage* 2008; 42: 635–48.
- Knowlton RC, Razdan SN, Limdi N, Elgavish RA, Killen J, Blount J, et al. Effect of epilepsy magnetic source imaging on intracranial electrode placement. *Ann Neurol* 2009; 65: 716–23.
- Kobayashi E, Bagshaw AP, Grova C, Dubeau F, Gotman J. Negative BOLD responses to epileptic spikes. *Hum Brain Mapp* 2006; 27: 488–97.
- Kobayashi E, Grova C, Tyvaert L, Dubeau F, Gotman J. Structures involved at the time of temporal lobe spikes revealed by interindividual group analysis of EEG/fMRI data. *Epilepsia* 2009; 50: 2549–56.
- Koenig T, Gianotti LRR. Scalp field maps and their characterization. Cambridge: Cambridge University Press; 2009.
- Lantz G, Spinelli L, Seeck M, de Peralta Menendez RG, Sottas CC, Michel CM. Propagation of interictal epileptiform activity can lead to erroneous source localizations: a 128-channel EEG mapping study. *J Clin Neurophysiol* 2003; 20: 311–9.
- Laufs H, Hamandi K, Salek-Haddadi A, Kleinschmidt AK, Duncan JS, Lemieux L. Temporal lobe interictal epileptic discharges affect cerebral activity in “default mode” brain regions. *Hum Brain Mapp* 2007; 28: 1023–32.
- Lazeyras F, Blanke O, Perrig S, Zimine I, Golay X, Delavelle J, et al. EEG-triggered functional MRI in patients with pharmacoresistant epilepsy. *J Magn Reson Imaging* 2000; 12: 177–85.
- Lehmann D, Skrandies W. Reference-free identification of components of checkerboard-evoked multichannel potential fields. *Electroencephalogr Clin Neurophysiol* 1980; 48: 609–21.
- Lehmann D, Skrandies W. Spatial analysis of evoked potentials in man—a review. *Prog Neurobiol* 1984; 23: 227–50.
- Lemieux L, Laufs H, Carmichael D, Paul JS, Walker MC, Duncan JS. Noncanonical spike-related BOLD responses in focal epilepsy. *Hum Brain Mapp* 2008; 29: 329–45.
- Lemieux L, Salek-Haddadi A, Josephs O, Allen P, Toms N, Scott C, et al. Event-related fMRI with simultaneous and continuous EEG: description of the method and initial case report. *Neuroimage* 2001; 14: 780–7.
- LeVan P, Gotman J. Independent component analysis as a model-free approach for the detection of BOLD changes related to epileptic spikes: a simulation study. *Hum Brain Mapp* 2009; 30: 2021–31.
- Liston AD, De Munck JC, Hamandi K, Laufs H, Ossenblok P, Duncan JS, et al. Analysis of EEG-fMRI data in focal epilepsy based on automated spike classification and Signal Space Projection. *Neuroimage* 2006; 31: 1015–24.
- Lopes da Silva FH. A critical review of clinical applications of topographic mapping of brain potentials. *J Clin Neurophysiol* 1990; 7: 535–51.
- Manganotti P, Formaggio E, Gasparini A, Cerini R, Bongiovanni LG, Storti SF, et al. Continuous EEG-fMRI in patients with partial epilepsy and focal interictal slow-wave discharges on EEG. *Magn Reson Imaging* 2008; 26: 1089–100.
- Mantini D, Perrucci MG, Del Gratta C, Romani GL, Corbetta M. Electrophysiological signatures of resting state networks in the human brain. *Proc Natl Acad Sci USA* 2007; 104: 13170–5.
- Marques JP, Rebola J, Figueiredo P, Pinto A, Sales F, Castelo-Branco M. ICA decomposition of EEG signal for fMRI processing in epilepsy. *Hum Brain Mapp* 2009; 30: 2986–96.
- Michel CM, Lantz G, Spinelli L, De Peralta RG, Landis T, Seeck M. 128-channel EEG source imaging in epilepsy: clinical yield and localization precision. *J Clin Neurophysiol* 2004a; 21: 71–83.
- Michel CM, Murray MM, Lantz G, Gonzalez S, Spinelli L, Grave de Peralta R. EEG source imaging. *Clin Neurophysiol* 2004b; 115: 2195–222.
- Moehring J, Moeller F, Jacobs J, Wolff S, Boor R, Jansen O, et al. Non-REM sleep influences results of fMRI studies in epilepsy. *Neurosci Lett* 2008; 443: 61–6.
- Moeller F, LeVan P, Gotman J. Independent component analysis (ICA) of generalized spike wave discharges in fMRI: comparison with general linear model-based EEG-fMRI. *Hum Brain Mapp* 2011; 32: 209–17.

- Moeller F, Tyvaert L, Nguyen DK, LeVan P, Bouthillier A, Kobayashi E, et al. EEG-fMRI: adding to standard evaluations of patients with non-lesional frontal lobe epilepsy. *Neurology* 2009; 73: 2023–30.
- Murray MM, Brunet D, Michel CM. Topographic ERP analyses: a step-by-step tutorial review. *Brain Topogr* 2008; 20: 249–64.
- Musso F, Brinkmeyer J, Mobascher A, Warbrick T, Winterer G. Spontaneous brain activity and EEG microstates. A novel EEG/fMRI analysis approach to explore resting-state networks. *Neuroimage* 2010; 52: 1149–61.
- Perrin F, Pernier J, Bertrand O, Echallier JF. Spherical splines for scalp potential and current density mapping. *Electroencephalogr Clin Neurophysiol* 1989; 72: 184–7.
- Perrin F, Pernier J, Bertrand O, Giard MH, Echallier JF. Mapping of scalp potentials by surface spline interpolation. *Electroencephalogr Clin Neurophysiol* 1987; 66: 75–81.
- Rathakrishnan R, Moeller F, Levan P, Dubeau F, Gotman J. BOLD signal changes preceding negative responses in EEG-fMRI in patients with focal epilepsy. *Epilepsia* 2010; 51: 1837–45.
- Ray A, Tao JX, Hawes-Ebersole SM, Ebersole JS. Localizing value of scalp EEG spikes: a simultaneous scalp and intracranial study. *Clin Neurophysiol* 2007; 118: 69–79.
- Rodionov R, De Martino F, Laufs H, Carmichael DW, Formisano E, Walker M, et al. Independent component analysis of interictal fMRI in focal epilepsy: comparison with general linear model-based EEG-correlated fMRI. *Neuroimage* 2007; 38: 488–500.
- Rosenow F, Luders H. Presurgical evaluation of epilepsy. *Brain* 2001; 124: 1683–700.
- Salek-Haddadi A, Diehl B, Hamandi K, Merschhemke M, Liston A, Friston K, et al. Hemodynamic correlates of epileptiform discharges: an EEG-fMRI study of 63 patients with focal epilepsy. *Brain Res* 2006; 1088: 148–66.
- Seeck M, Lazeyras F, Michel CM, Blanke O, Gericke CA, Ives J, et al. Non-invasive epileptic focus localization using EEG-triggered functional MRI and electromagnetic tomography. *Electroencephalogr Clin Neurophysiol* 1998; 106: 508–12.
- Spencer S, Huh L. Outcomes of epilepsy surgery in adults and children. *Lancet Neurol* 2008; 7: 525–37.
- Sperli F, Spinelli L, Seeck M, Kurian M, Michel CM, Lantz G. EEG source imaging in pediatric epilepsy surgery: a new perspective in presurgical workup. *Epilepsia* 2006; 47: 981–90.
- Tao JX, Ray A, Hawes-Ebersole S, Ebersole JS. Intracranial EEG substrates of scalp EEG interictal spikes. *Epilepsia* 2005; 46: 669–76.
- Thornton R, Laufs H, Rodionov R, Cannadathu S, Carmichael DW, Vulliemoz S, et al. EEG correlated functional MRI and postoperative outcome in focal epilepsy. *J Neurol Neurosurg Psychiatry* 2010a; 81: 922–7.
- Thornton RC, Rodionov R, Laufs H, Vulliemoz S, Vaudano A, Carmichael D, et al. Imaging haemodynamic changes related to seizures: comparison of EEG-based general linear model, independent component analysis of fMRI and intracranial EEG. *Neuroimage* 2010b; 53: 196–205.
- Van De Ville D, Britz J, Michel CM. EEG microstate sequences in healthy humans at rest reveal scale-free dynamics. *Proc Natl Acad Sci USA* 2010; 107: 18179–84.
- Vulliemoz S, Carmichael DW, Rosenkranz K, Diehl B, Rodionov R, Walker MC, et al. Simultaneous intracranial EEG and fMRI of interictal epileptic discharges in humans. *Neuroimage* 2011; 54: 182–90.
- Vulliemoz S, Lemieux L, Daunizeau J, Michel CM, Duncan JS. The combination of EEG source imaging and EEG-correlated functional MRI to map epileptic networks. *Epilepsia* 2010; 51: 491–505.
- Vulliemoz S, Rodionov R, Carmichael DW, Thornton R, Guye M, Lhatoo SD, et al. Continuous EEG source imaging enhances analysis of EEG-fMRI in focal epilepsy. *Neuroimage* 2009a; 49: 3219–29.
- Vulliemoz S, Thornton R, Rodionov R, Carmichael DW, Guye M, Lhatoo S, et al. The spatio-temporal mapping of epileptic networks: combination of EEG-fMRI and EEG source imaging. *Neuroimage* 2009b; 46: 834–43.
- Webber WR, Litt B, Wilson K, Lesser RP. Practical detection of epileptiform discharges (EDs) in the EEG using an artificial neural network: a comparison of raw and parameterized EEG data. *Electroencephalogr Clin Neurophysiol* 1994; 91: 194–204.
- Zijlmans M, Huiskamp G, Hersevoort M, Seppenwoolde JH, van Huffelen AC, Leijten FS. EEG-fMRI in the preoperative work-up for epilepsy surgery. *Brain* 2007; 130: 2343–53.